Supplementary Materials for

Cytoplasmic protein granules organize kinase-mediated RAS signaling

Asmin Tulpule[#,1], Juan Guan[#,2], Dana S. Neel[#,3], Yone Phar Lin[1], Ann Heslin[1], Hannah Allegakoan[1], Shriya Perati[1], Alejandro D. Ramirez[2], Xiaoyu Shi[2], Bin Yang[2], Siyu Feng[4], Bo Huang[2, 5, 6, *], Trever G. Bivona[3,*]

Correspondence to: Trever G. Bivona MD PhD (email: trever.bivona@ucsf.edu) or Bo Huang PhD (email: bo.huang@ucsf.edu)

This PDF file includes:

Materials and Methods
Supplementary Notes 1 and 2
Figs. S1 to S24

Materials and Methods:

Cell line generation

Generation of endogenously tagged mNeonGreen2$_{1\text{-}10/11}$ cell lines was performed in the human bronchial epithelial cell line (Beas2B) and the patient-derived oncogenic ALK cell line (H3122) as previously described [21]. Correct integration of mNeonGreen2$_{11}$ was confirmed by genomic sequencing and by reduction in fluorescence upon gene knockdown. sgRNA spacer sequences used in this study are shown below.

GRB2: CTTAGACGTTCCGGTTCACG
SOS1: ACAGAGGAACTCAGGAAGAA
GAB1: GCGAAACCGTCCATCTTGCG
KRAS: AATGACTGAATATAAACTTG
HRAS: GATGACGGAATATAAGCTGG
NRAS: AATGACTGAGTACAAACTGG
ARAF: GGCTCCATGGAGCCACCACG
BRAF: GGCTCTCGGTTATAAGATGG
CRAF: GCATCAATGGAGCACATACA

Cell line maintenance

All cell lines were maintained in humidified incubators with 5% CO2 at 37 °C. Beas2B and endogenously tagged derivatives, as well as the patient derived cancer cell lines H3122, STE-1, and HCC827 were cultured in RPMI-1640 medium supplemented with 10% FBS and penicillin-streptomycin at 100 µg/mL. 293T cells were cultured in DMEM-High Glucose supplemented with 10% FBS and 100 µg/mL of penicillin/streptomycin. All cell lines were tested for mycoplasma every 3 months using MycoAlert Mycoplasma Detection Kit (Lonza, Basel, Switzerland). All cells used were < 20 passages from thaw.

Biochemical fractionation

Cells were seeded in 10 cm dishes and harvested the following day by scraping into buffer A [10 mM Tris-HCl (pH 7.4), 1 mM EDTA, 250 mM Sucrose, supplemented with 1X HALT protease inhibitors (Thermo Fisher Scientific)]. Lysates were gently sonicated on minimum intensity and cleared by centrifugation. Lysate was then split equivalently to two ultracentrifugation tubes, and one tube was supplemented with 1% Triton X-100. Lysates were then ultracentrifuged at 100,000×g for 1 hour at 4 °C in an Optima MAX Ultracentrifuge (Beckman Coulter, Brea, CA). Supernatant and pelleted fractions were separated, resuspended with Laemmli sample buffer, boiled, and analyzed by SDS-PAGE.

Antibodies and immunoblotting

Antibodies against the following were obtained from Cell Signaling Technology (Danvers, MA, USA) and were used at a dilution of 1:1000: ALK (C26G7), p-Y1604-ALK (#3341), ERK1/2 (#3493), p-T202/Y204-ERK1/2 D13.14.4e (#4370), DCP1B (D2P9W), EEA1 (C45B10), EGF Receptor (D38B1) XP, p-Y1068-EGF Receptor (D7A5) XP, MEK1/2 (9122), p-S221-MEK1/2 (166F8), RET (C31B4), p-Y905-RET (#3221), horseradish peroxidase (HRP)-conjugated anti-mouse (#7076) and HRP-conjugated anti-rabbit (#7074). Antibodies to the following were obtained from Santa Cruz Biotechnologies (Santa Cruz, CA, USA): actin (I19, 1:1000 dilution), HRAS (C-20, 1:200 dilution), NRAS (F155, 1:200 dilution), KRAS (F234, 1:500 dilution),

Calnexin Antibody (AF18), ARAF (sc-135820, 1:1000), BRAF (F7, 1:1000), CRAF (E10, 1:1000), GRB2 (C7: 1:1000). Anti-Ras antibody, clone 10 (1:1000) was obtained from EMD Millipore (Hayward, CA) and anti-FLAG M2 monoclonal antibody was obtained from Sigma (USA).

For immunoblotting, cells were serum-starved (0% serum for 24 hours), then washed with ice-cold PBS and scraped in ice cold RIPA buffer [25 mM Tris·HCl (pH 7.6), 150 mM NaCl, 1% NP-40, 1% sodium deoxycholate, 0.1% SDS, supplemented with 1X HALT protease inhibitor cocktail and 1X HALT phosphatase inhibitor cocktail (Thermo Fisher Scientific)]. Lysates were clarified with sonication and centrifugation. Lysates were subject to SDS/PAGE followed by blotting with the indicated antibodies. Signal was detected using Amersham ECL Prime reagent (GE Healthcare Life Sciences, Chicago, IL, USA) and chemiluminescence on an ImageQuant LAS 4000 (GE Healthcare Life Science, Chicago, IL, USA).

Generation of stable cell lines expressing wild-type or cytosolic RAS
293T cells were infected with wild-type H/N/KRAS or respective cytosolic RAS mutants (KRAS C185S, HRAS C186S, NRAS C186S) then selected with puromycin to generate stable cell lines. RAS activation assays were performed 48 hours after transfection of empty vector, EML4-ALK, or oncogenic EGFR (EGFR L858R). H3122 and HCC827 cell lines were also infected with wild-type and C185S KRAS and selected with puromycin to generate stable cell lines. RAS activation assays were performed comparing 2 hour treatment with 100 nM crizotinib in H3122 cells or 100 nM erlotinib in HCC827 cells with mock DMSO treatment.

Compounds
Crizotinib and erlotinib were purchased from Selleck Chemicals (Houston, TX) and resuspended in DMSO.

RAS activation assays
The RAS GST-RBD activation kit was obtained from Cytoskeleton (Denver, CO, USA; #BK008). The protocol was according to the manufacturer's instructions. Lysis buffer for RAS-GTP pulldowns was 50 mM Tris (pH 7.5), 10 mM $MgCl_2$, 0.5 M NaCl, and 2% Igepal. 150 µg of lysate was incubated with 10µl RBD-beads overnight, followed by Western blotting. RAS-GTP levels were normalized to total RAS protein levels.

Live-cell microscopy
Cells were seeded in 35mm glass-bottom dishes (MatTek, Ashland, MA) or 8-well Nunc Lab-Tek 8 well imaging chambers (Thermo Fisher Scientific) and then imaged using a Nikon Ti microscope with a CSU-W1 spinning disk confocal using a 100X/1.4 Plan Apo VC objective (Nikon Imaging Center, UCSF). Images were acquired on MicroManager software and analyzed using ImageJ software.

Structured illumination microscopy
Beas2B cells were seeded into Nunc Lab-Tek 8-well imaging chambers and eYFP::EML4-ALK was transfected via Mirus TransIT-LT1 (Mirus Bio LLC, Madison, WI, USA). 24 hours later, both live cells and fixed cells were imaged with structured illumination microscopy on a DeltaVision OMX imaging system (GE Healthcare) in 3D-SIM mode. The procedure for cell

fixation was 4% paraformaldehyde incubation for 5 minutes followed by three PBS washes. The 3D structures of granules were rendered with visualization software Chimera X.

Fluorescence recovery after photobleaching

For photobleaching experiments, Beas2B cells were seeded into Nunc Lab-Tek 8-well imaging chambers and transfected with mTagBFP2::EML4-ALK via Mirus TransIT-LT1. A 473 nm laser (Rapp Optoelectronic) at excitation intensity of 30 mW was used to photobleach regions of interest (ROIs) corresponding to individual granules in the sample. The fluorescence intensity was monitored before and after photobleaching with time interval of 3 seconds. Further intensity analyses were done in MatLab with custom-written code.

Monitoring granules during hexanediol treatment

Beas2B cells expressing tagBFP::EML4-ALK were seeded into Nunc Lab-Tek 8-well imaging chambers. A custom-made sample holder ensured the imaging chamber fits securely on the microscope stage without position shift. The cells were first imaged in regular RPMI cell culture media and then the media was replaced by RPMI media containing 10% hexanediol (Sigma). The same field of view was monitored at defined time points after addition of hexanediol.

Quantification of co-localization between EML4-ALK granules and endogenous signaling proteins

Customized MatLab code was written to correct for uneven illumination pattern in the optical path and cell autofluorescence background. Granules were identified with Cellprofiler feature-finding module using Otsu thresholding method and size constraint from 0.4 to 2 μm in diameter. The pair-wise centroid distance between features in BFP and GFP channels, corresponding to EML4-ALK granules and signaling proteins respectively, were calculated to identify co-localization events. Typically, ~20 images containing 30+ cells and ~300 granules for each signaling protein were analyzed in an automated batch-processing format. All co-localization events were confirmed manually by overlaying identified features with raw images.

Quantification of enrichment level of signaling proteins at EML4-ALK granules

Customized MatLab code was written to identify pixels corresponding to EML4-ALK granules in the BFP channel in a given image. The intensity in the GFP channel at the positions of these pixels, corresponding to the enriched signaling proteins, was averaged for individual granules. The ratio of the average pixel intensity at the granule to the pixel intensity averaged over the whole cell area is the fold enrichment of the signaling protein at each granule.

Quantification of fraction of granule containing cells for EML4-ALK and CCDC6-RET mutants

Beas2B cells were seeded into Nunc Lab-Tek 8-well imaging chambers and plasmids encoding wild-type and mutant forms of tagBFP::EML4-ALK (i.e. ΔTD, ΔHELP, K589M, see text for details) and tagBFP::CCDC6-RET (i.e. ΔCC, K147M) were transfected using Mirus TransIT-LT1. 24 hours later, an initial position in each well was randomly picked as the center of an area of 650 μm x 650 μm and imaged with automated scanning and tiling done through MicroManager with a 100x oil objective (N.A. = 1.40). The process was repeated three times and all the cells were scored manually to determine if they contained cytoplasmic granules.

Immunoprecipitation
For immunoprecipitation assays, HEK 293T cells were transfected with FLAG-tagged versions of EML4-ALK and respective mutants. 48 hours post-transfection (after serum starvation in 0% serum for 24 hours), the cells were resuspended in lysis buffer (0.5% NP-40, 150 mM NaCl, 50 mM Tris.Cl, pH 7.5) containing protease and phosphatase inhibitor cocktails (Sigma). Lysates were syringed and centrifuged to clarify, then whole-cell extracts were incubated overnight with M2 agarose-FLAG beads (Sigma) at 4°C. The immunocomplexes were washed three times with wash buffer (50 mM Tris (pH 7.4, 150 mM NaCl) and FLAG beads were boiled and loaded for SDS-PAGE.

Immunofluorescence
H3122 or Beas2B cells expressing EML4-ALK were seeded in 4-well Lab Tek II Chamber Slides (Thermo Fisher Scientific). The following day, cells were fixed for 15 minutes with 4% paraformaldehyde, washed, and incubated in blocking buffer for 1 hour (1X PBS with 1% BSA and 0.3% Triton-X100). Blocking buffer was aspirated and cells were incubated with primary antibody (either ALK DF53 1:1000 from Cell Signaling Technology or FLAG-M2 1:1000 from Sigma) overnight in the dark at 4 °C. The following day, cells were washed, incubated with fluorophore-conjugated secondary antibodies (Alexa Fluor 488/594 from Abcam, 1:2000) for 1 hour at room temperature in the dark, washed, and then mounted using ProLong Gold Antifade reagent with DAPI (Cell Signaling Technology). Slides were analyzed using a Nikon Ti microscope with a CSU-W1 spinning disk confocal using a 100 × 1.4 NA Plan Apo VC objective (Nikon Imaging Center, UCSF). Images were acquired on MicroManager software and analyzed using ImageJ software.

siRNA
Transfection of siRNA was performed with Dharmafect reagent (Dharmacon, USA). Smartpool siRNA used in experiments were directed against GRB2, SOS1, ARAF, BRAF, and CRAF and were purchased from Dharmicon and used according to the manufacturer's protocol.

Plasmids and construct generation
cDNA sequences for GRB2, ARAF, BRAF, and CRAF were cloned into the mEGFP-C1 vector. EML4-ALK cDNA and respective mutants were cloned into pBabe-puro with a N-terminal FLAG tag and mTagBFP2-C1. EGFRL858R was cloned into pBabe-puro and mTagBFP2-N1. All mutants were generated through a combination of QuikChange site-directed mutagenesis (Agilent) and gene synthesis (Genewiz).The mutants contain the following modifications:

EML4-ALK full-length sequence GenBank: AB274722.1, using cDNA from bases 271 – 3450, mutations/deletions based on this sequence numbering. EML4-ALK kinase-deficient K589M: A2036T, EML4-ALK ΔHELP: deletion of bases 928-1158, EML4-ALK ΔTD: deletion of bases 310-459. CCDC6-RET full-length sequence GenBank: KU254649.1, cDNA from bases 1-1512, mutations/deletions based on this sequence numbering. CCDC6-RET kinase-deficient K147M: A440T, CCDC6-RET ΔCC: deletion of bases 160-303.

DNA transfections
293T and Beas2B cells were transiently transfected using Mirus TransIt-LT1 transfection reagent according to manufacturer's protocol.

Viral transduction
cDNA's for EML4-ALK, KRAS, HRAS, NRAS and respective cytosolic mutants were cloned into pLV-EF1a-IRES-blast (or hygromycin/puromycin selectable equivalent vectors). HEK 293T viral packaging cells were plated in 10 cm dishes the day prior to transfection. They were transfected with lentiviral or retroviral expression constructs and the appropriate packaging plasmids using Mirus TransIt-LT1 transfection reagent. Viral supernatants were collected 48-72 hours post-transfection and used to transduce cell lines in the presence of 1× Polybrene for 24 hours.

Statistical analysis
P values were determined with unpaired *t*-tests between comparator groups using GraphPad software.

Supplementary Notes:

Supplementary Note #1: RAS proteins are synthesized on free polysomes in the cytosol and become peripherally-associated with lipid-membrane compartments (ER, Golgi, PM) via a series of post-translational modifications that are directed by the C-terminal-CAAX motif and hypervariable domain [S1]. Lipid membrane association of RAS GTPase (H/N/K isoforms) has been shown to be both necessary and sufficient for downstream RAF/MEK/ERK activation in the context of both normal cells and cancer [13, 14]. Despite this established principle, quantitative studies established that a substantial pool of cytosolic RAS proteins exists in mammalian cells, albeit with unclear functional significance [22].

In the current understanding of RAS signaling at the PM, RAS proteins are not substantially recruited en masse to subcellular structures such as lipid membranes upon RTK activation but instead are membrane-resident and become GTP-bound locally *in situ* (although lipid-membrane microdomain movement of RAS GTPases [1, 35] during signaling can occur) [24-26].

The majority of the endogenous cytoplasmic RAS pool exists in a prenylated (farnesylated) state that is either *en route* to the PM or recycling between the PM and endomembranes [S2, 22]. The well-studied cytosolic RAS mutants (i.e. "SAAX" mutants KRAS C185S, HRAS C186S, NRAS C186S) are incapable of undergoing the initial farnesylation step in RAS trafficking and thus do not associate with lipid membranes (either internal or PM) [14]. These mutants provide a useful experimental tool to measure activation of cytosolic RAS in the absence of lipid. In addition to lipid membrane targeting, farnesylation of RAS is needed for RAS to promote RAF activation [S3, S4]. Therefore, non-farnesylated "SAAX" mutants of RAS are incompetent to promote productive downstream RAF/MEK/ERK signaling.

Supplementary Note #2: RAF protein recruitment to subcellular structures (i.e. PM) and subsequent downstream MAPK pathway activation requires local RAS-GTP accumulation [S5]. For the RAF reporter assay, we observed the expected PM recruitment of exogenous fluorescent protein-tagged RAF isoforms (A/B/C) upon oncogenic KRAS expression (Fig. S10). In contrast, Beas2B cell lines with endogenous mNeonGreen2-tagging of A/B/CRAF did not reliably display PM recruitment of RAF proteins above baseline auto-fluorescence upon oncogenic KRAS expression (Fig. S11). This finding likely reflects a known limitation of fluorescence tagging of genes at endogenous loci that can occur on a case by case basis, especially for genes that express at low levels as we described previously [S6].

Supplementary References:

1. Cox, A.D., C.J. Der, and M.R. Philips, *Targeting RAS Membrane Association: Back to the Future for Anti-RAS Drug Discovery?* Clin. Cancer Res., 2015. **21**(8): p. 1819-1827.
2. Schmick, M., et al., *KRas Localizes to the Plasma Membrane by Spatial Cycles of Solubilization, Trapping and Vesicular Transport.* Cell, 2014. **157**(2): p. 459-471.
3. Stokoe, D. and F. McCormick, *Activation of c-Raf-1 by Ras and Src through different mechanisms: activation in vivo and in vitro.* Embo j, 1997. **16**(9): p. 2384-96.
4. Williams, J.G., et al., *Elucidation of binding determinants and functional consequences of Ras/Raf-cysteine-rich domain interactions.* J Biol Chem, 2000. **275**(29): p. 22172-9.

5. Lavoie, H. and M. Therrien, *Regulation of RAF protein kinases in ERK signalling.* Nat. Rev. Mol. Cell Biol., 2015. **16**: p. 281.
6. Leonetti, M.D., et al., *A scalable strategy for high-throughput GFP tagging of endogenous human proteins.* Proc Natl Acad Sci USA, 2016. **113**(25): p. E3501-E3508.

Supplementary Figures:

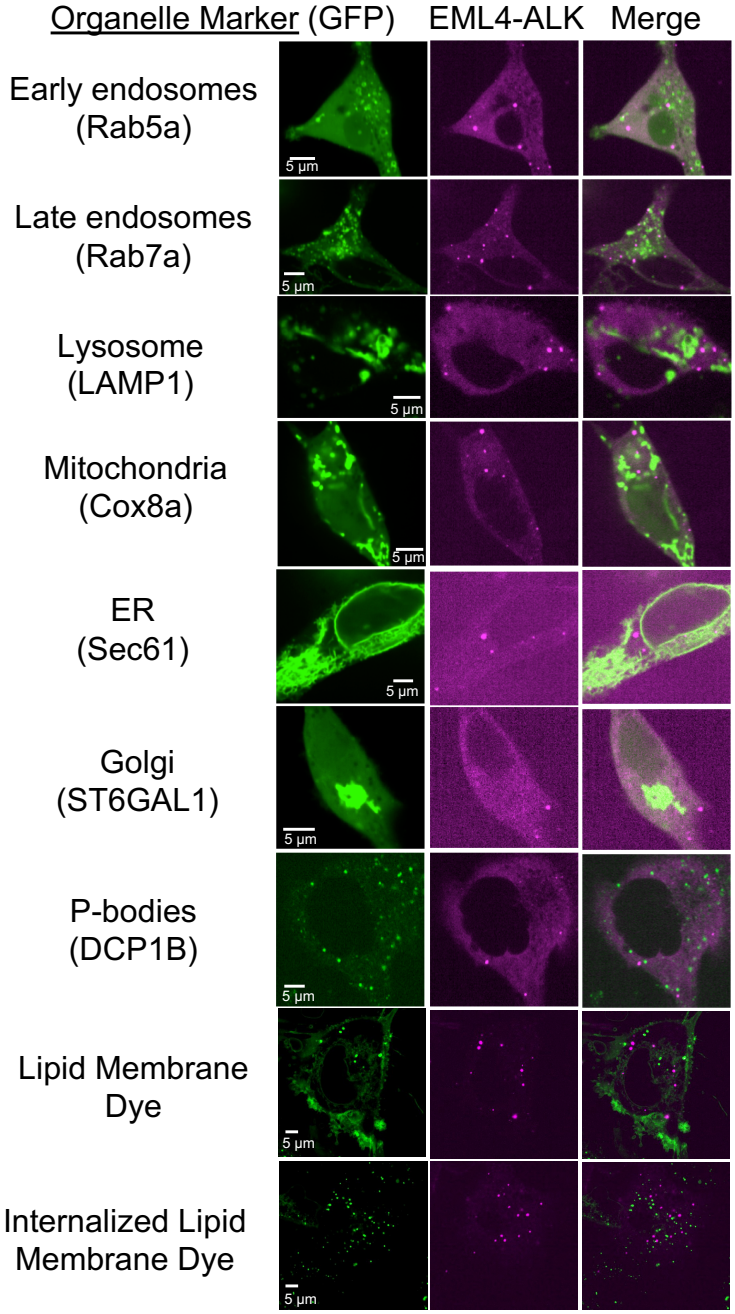

Figure S1: EML4-ALK puncta do not co-localize with lipid membrane containing intracellular structures. Live-cell confocal imaging of human epithelial cell line Beas2B upon expression of fluorescently tagged EML4-ALK (mTagBFP2) and mEGFP-tagged organelle markers as listed. Membrane dye experiments were conducted using live cells incubated with CellTracker™ CM-DiI Dye (Invitrogen) according to manufacturer's recommended protocol. Each panel is a representative image of at least 20 analyzed cells per condition in 3 independent experiments.

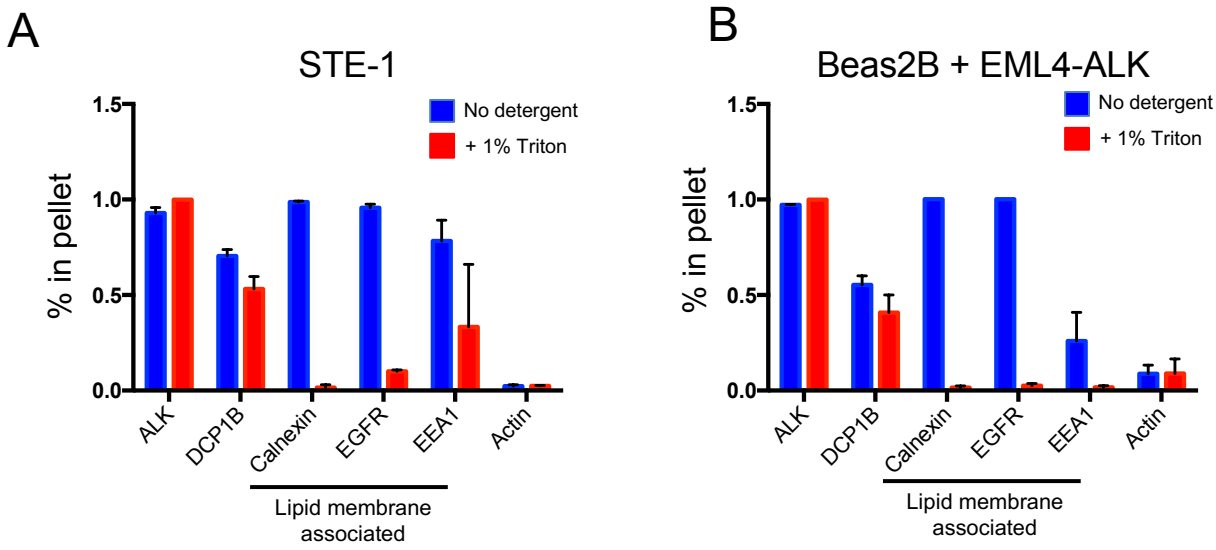

Figure S2: EML4-ALK subcellular fractionation is not affected by lipid solubilizing detergents. Subcellular fractionation by ultracentrifugation +/– detergent (1% Triton X-100) to disrupt lipid membranes in STE-1 (A), an EML4-ALK expressing cancer cell line, and Beas2B cells expressing EML4-ALK (B). In both cell lines, EML4-ALK and DCP1B are statistically distinct ($p < 0.01$ for all comparisons) from the lipid membrane-associated proteins, which shift from the insoluble fraction (pellet) to the soluble fraction with detergent. Bar graphs reflect quantification of Western blotting results for 3 independent replicates. Percent in pellet calculated as ratio of the insoluble to soluble fractions as assessed by Western blotting. Error bars represent ± SEM.

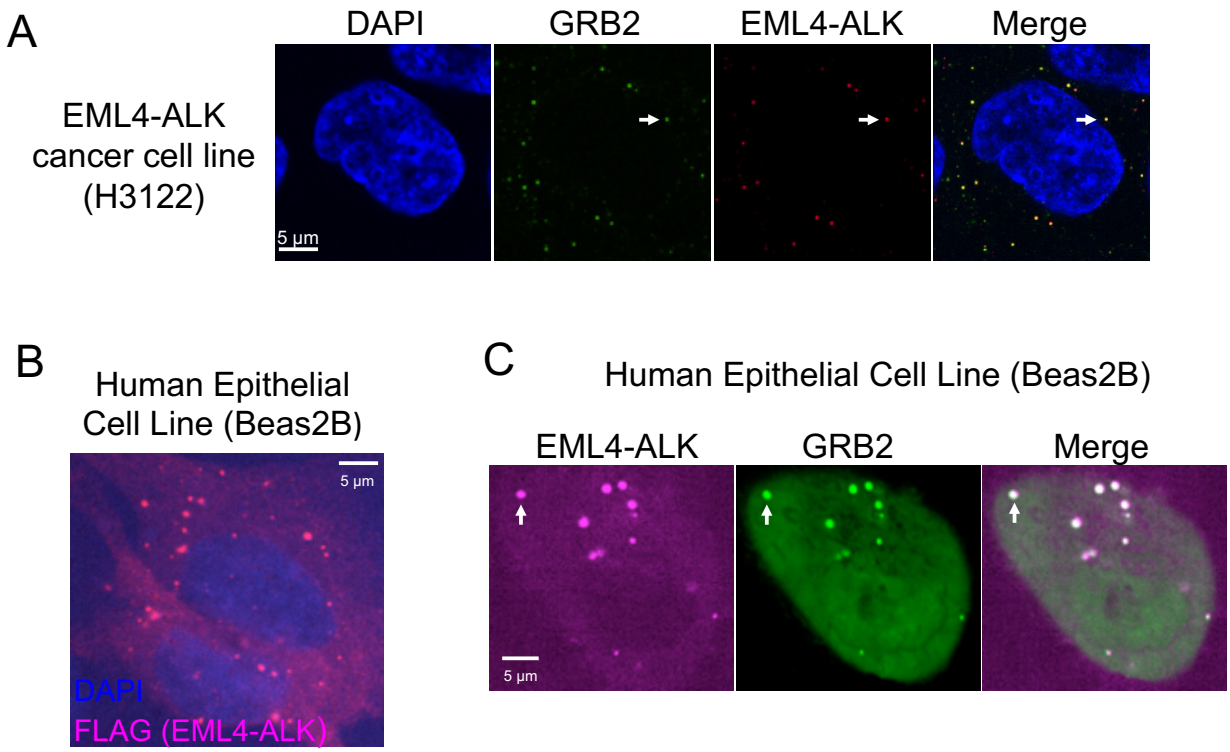

Figure S3: GRB2 is recruited to EML4-ALK granules in patient derived cancer cells. (A) Immunofluorescence images using an anti-ALK antibody to detect endogenous expression of EML4-ALK in a patient-derived cancer cell line (H3122) with endogenous mNeonGreen2-tagging of GRB2. (B) Anti-FLAG immunofluorescence of FLAG tagged EML4-ALK expressed in human epithelial cell line Beas2B. (C) Live-cell confocal imaging of mTagBFP2::EML4-ALK and mEGFP::GRB2 upon dual expression in Beas2B cells. For all panels (A-C), images are representative of 50-100 analyzed cells in total over 3 independent experiments. White arrows indicate a representative EML4-ALK cytoplasmic protein granule with local enrichment of GRB2 (multiple non-highlighted granules also show colocalization between EML4-ALK and GRB2).

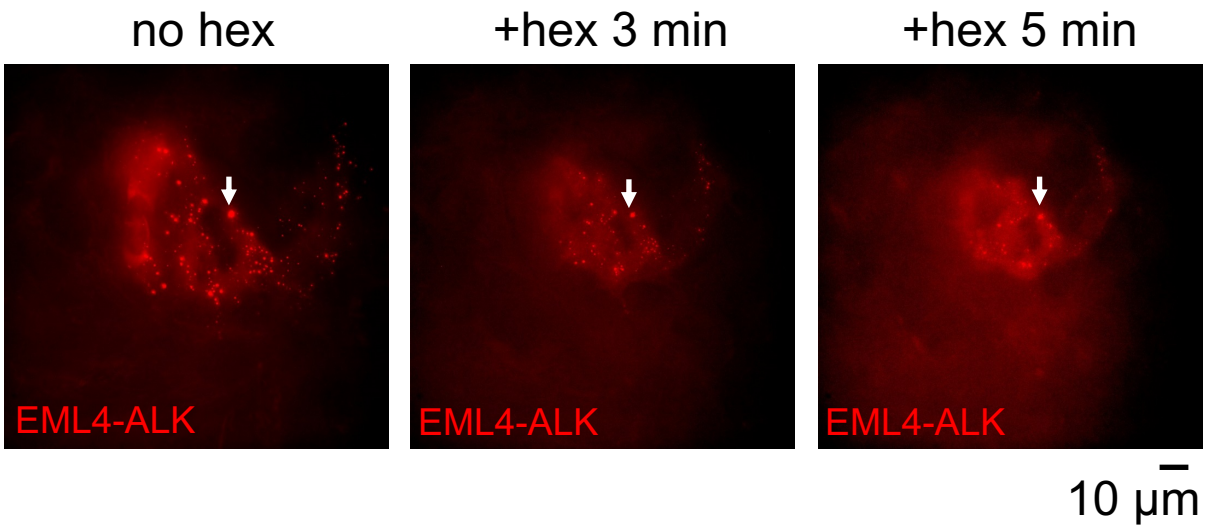

Figure S4: EML4-ALK granules are not disrupted by hexanediol. Live-cell imaging of human epithelial cell line Beas2B expressing mTagBFP2::EML4-ALK and then treated with hexanediol (hex) and imaged at respective time points. Images are representative of at least 5 analyzed cells in 3 independent experiments. White arrows indicate a representative EML4-ALK cytoplasmic protein granule (multiple non-highlighted granules are also pictured in all panels).

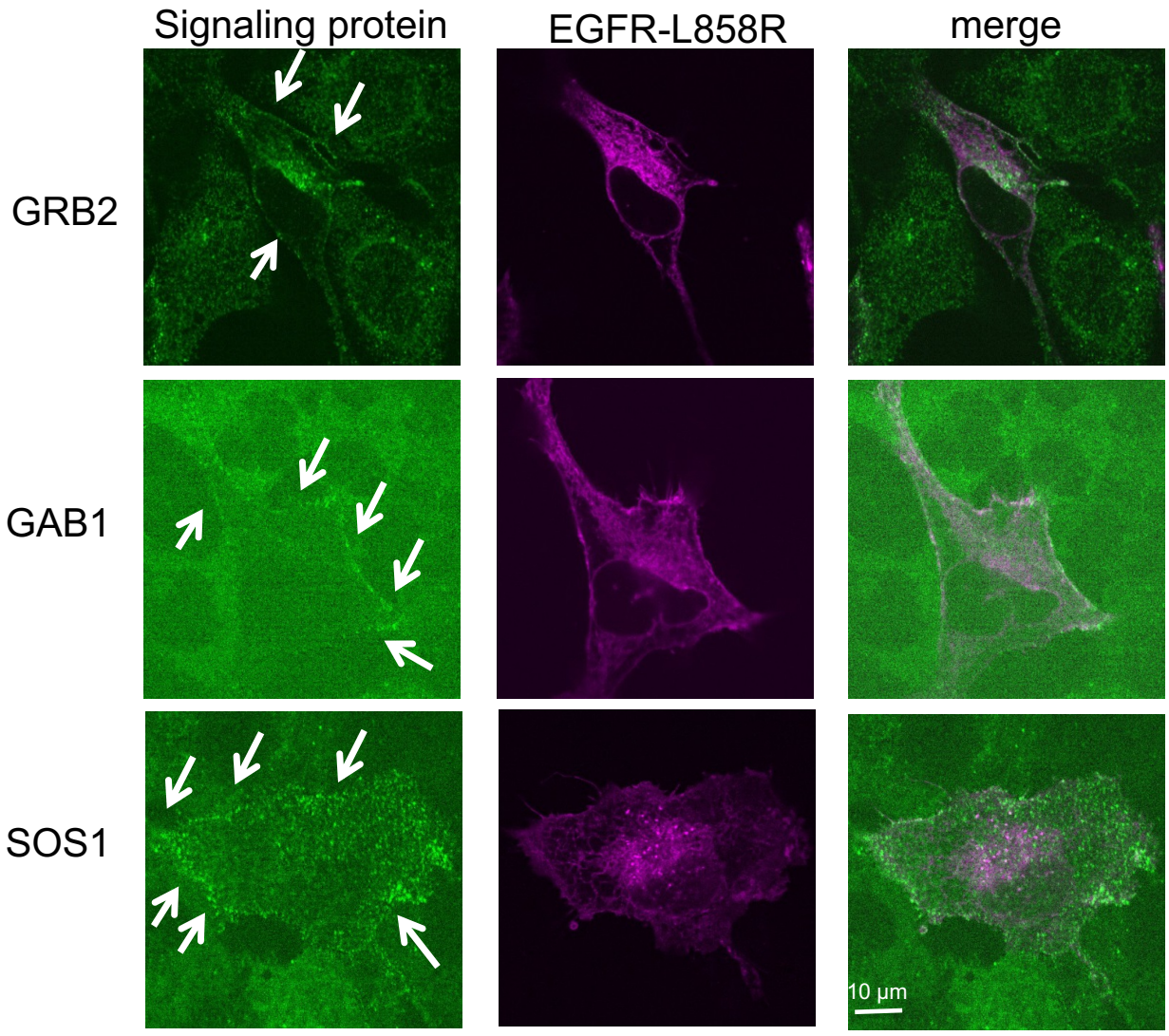

Figure S5: Oncogenic EGFR recruits endogenously tagged RAS adaptors to the PM. (A-C) Live-cell confocal imaging of mTagBFP2::EGFR L858R (oncogenic EGFR) expressed in human epithelial cell lines (Beas2B) with endogenous mNeonGreen2-tagging of GRB2, GAB1, and SOS1. Arrows denote plasma membrane enrichment of GRB2, GAB1, and SOS1. Representative images from at least 30 cells analyzed per condition in 3 independent experiments.

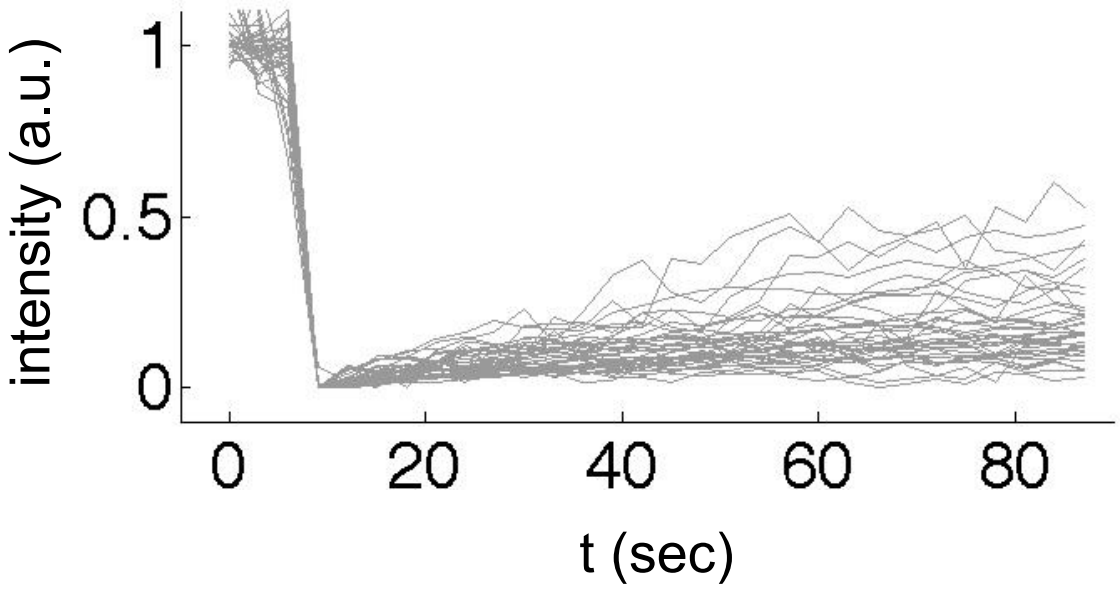

Figure S6: FRAP analysis of GRB2 protein displays slow-recovery and heterogeneity between individual granules. FRAP experiments performed in human epithelial cells (Beas2B) with endogenous mNeonGreen2-tagging of GRB2, upon expression of mTagBFP2::EML4-ALK. Graph displays individual recovery of fluorescence intensity after photobleaching of GRB2 enriched at EML4-ALK granules, t denotes time in seconds, intensity in arbitrary units (a.u.) normalized to 1. N = 30 cells.

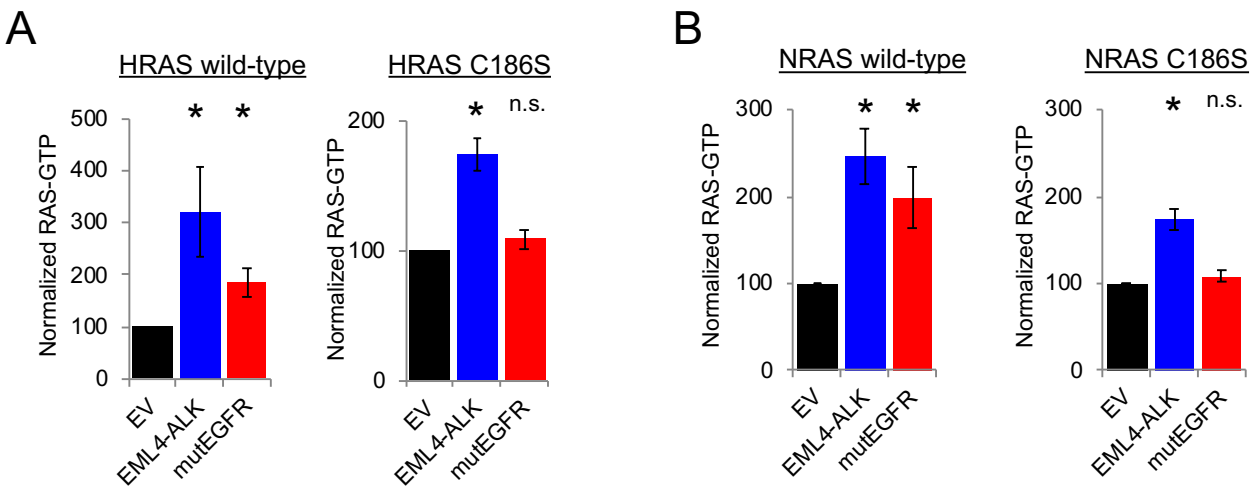

Figure S7: EML4-ALK specific activation of cytosolic RAS. (A, B) HRAS/NRAS wild-type or cytosolic mutants (HRAS C186S, NRAS C186S) were stably expressed in 293T cells and then transfected with either empty vector (EV), EML4-ALK, or oncogenic EGFR-L858R (mutEGFR). RAS-GTP levels were normalized to the relevant total RAS protein level (H/NRAS wild-type or C186S). N = 4. Error bars represent ± SEM, * denotes p value < 0.05, n.s. denotes non-significant comparison.

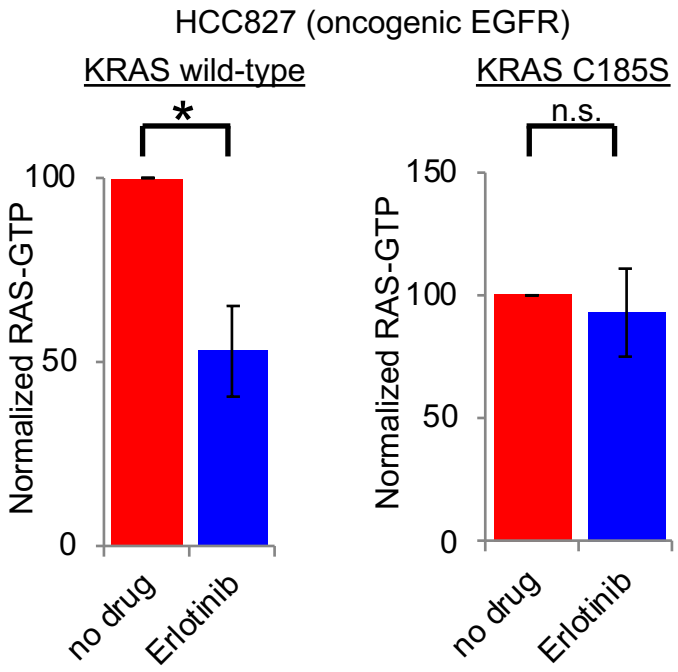

Figure S8: EGFR inhibitor treatment reduces wild-type, but not cytosolic, RAS-GTP levels in an EGFR mutant cancer cell line. Patient-derived oncogenic EGFR expressing cell line (HCC827) with stable expression of either wild-type KRAS or cytosolic mutant (KRAS C185S). RAS-GTP levels determined +/– two hours of 100 nM erlotinib treatment and normalized to the relevant total RAS protein level (KRAS wild-type or C185S). N = 4. Error bars represent ± SEM, * denotes p value < 0.05, n.s. denotes non-significant comparison.

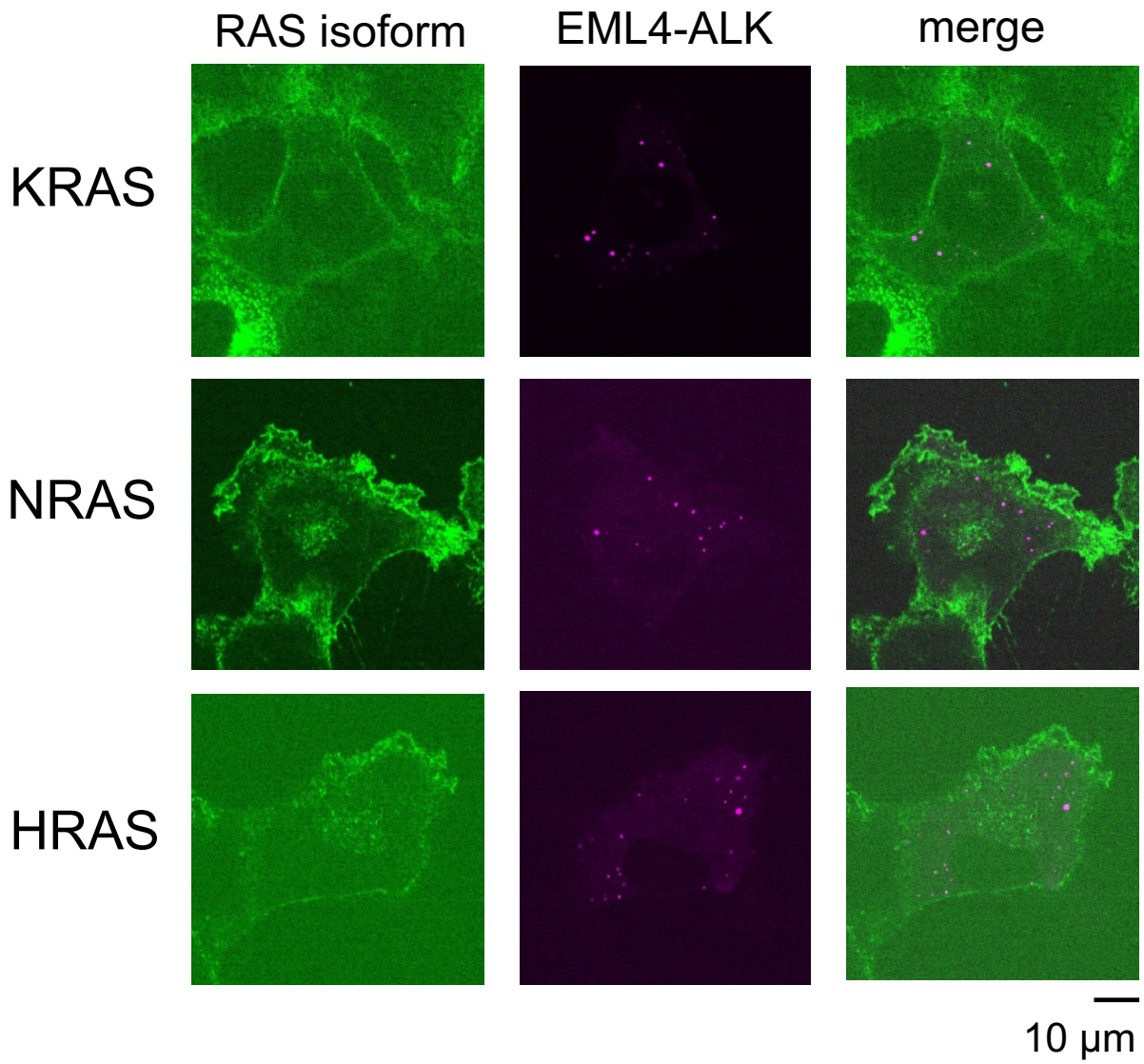

Figure S9: Endogenously tagged RAS isoforms do not enrich at EML4-ALK granules. Live-cell confocal imaging of mTagBFP2::EML4-ALK expressed in human epithelial cell lines (Beas2B) with endogenous mNeonGreen2-tagging of KRAS, NRAS, and HRAS. Images are representative of at least 20 analyzed cells per condition in 3 independent experiments with no co-localization observed between RAS isoforms and EML4-ALK granules.

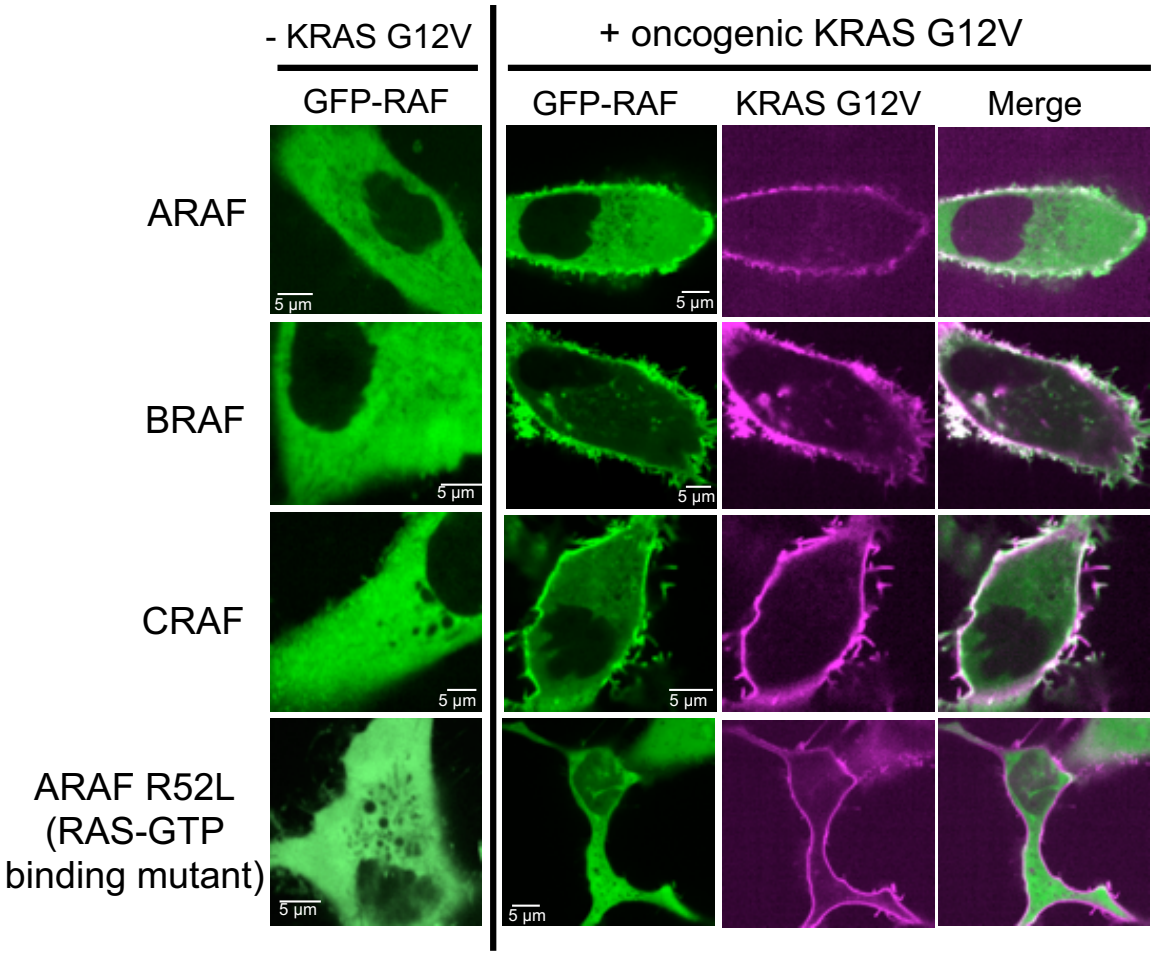

Figure S10: GFP tagged RAF isoforms enrich at the PM in setting of oncogenic KRAS. Live-cell confocal imaging of human epithelial cell line Beas2B transfected with mEGFP-labelled ARAF/BRAF/CRAF and ARAF R52L, a mutant form of ARAF with reduced binding to RAS-GTP. Left column demonstrates baseline RAF protein localization pattern and right three panels show plasma membrane re-localization of A/B/CRAF proteins, but not ARAF R52L, upon expression of mTagBFP2::KRAS G12V (oncogenic KRAS). Images are representative of 15-25 cells analyzed per condition in 3 independent experiments.

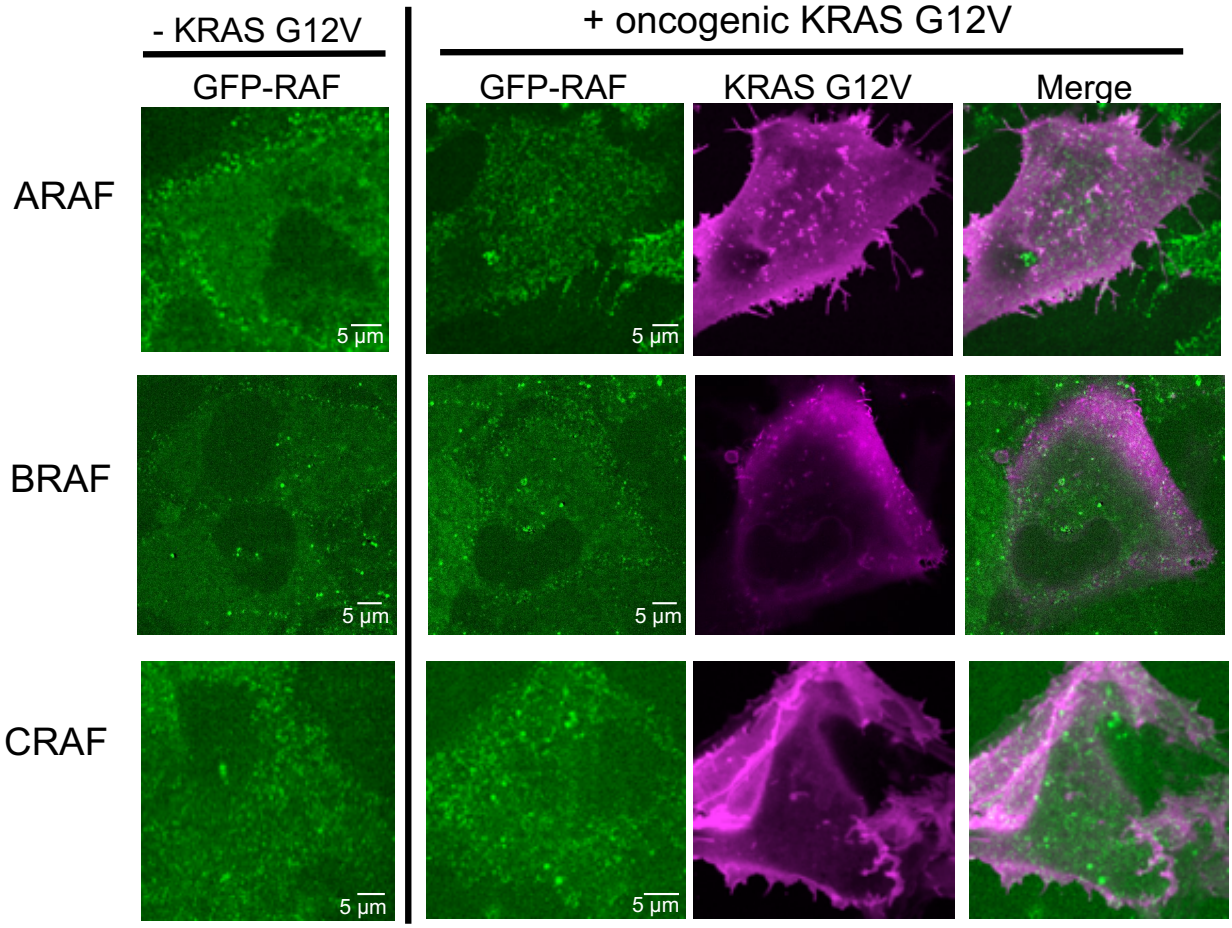

Figure S11: Endogenously tagged RAF isoforms do not significantly enrich at the PM in setting of oncogenic KRAS. Live-cell confocal imaging of human epithelial cell lines (Beas2B) with endogenous mNeonGreen2-tagging of ARAF, BRAF, and CRAF. Left column shows baseline RAF protein localization pattern and right three panels show lack of PM re-localization upon expression of mTagBFP2::KRAS G12V (oncogenic KRAS). Images are representative of at least 75 cells analyzed per condition in total over 3 independent experiments.

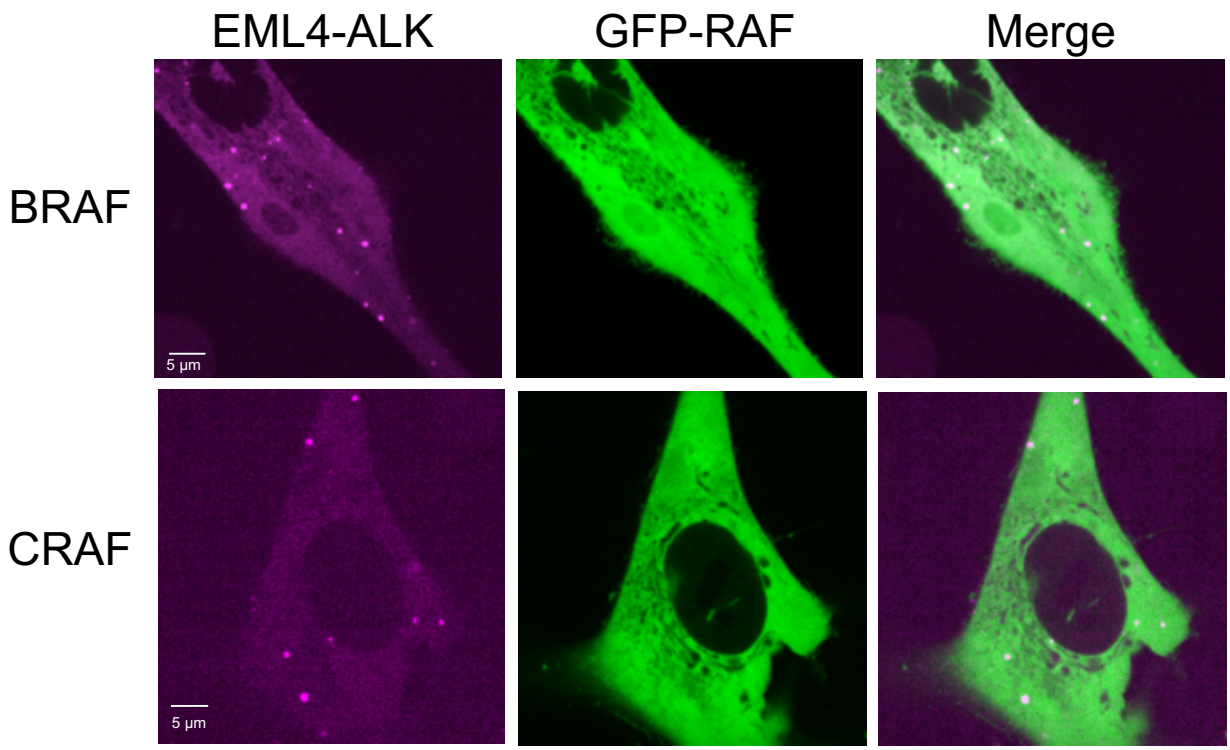

Figure S12: EML4-ALK protein granules do not locally recruit BRAF or CRAF. Live-cell confocal imaging of human epithelial cell line Beas2B expressing mTagBFP2::EML4-ALK and mEGFP-labelled BRAF or CRAF. Images are representative of at least 100 cells in total analyzed per condition over 3 independent experiments with no cells demonstrating BRAF or CRAF co-localization with EML4-ALK granules.

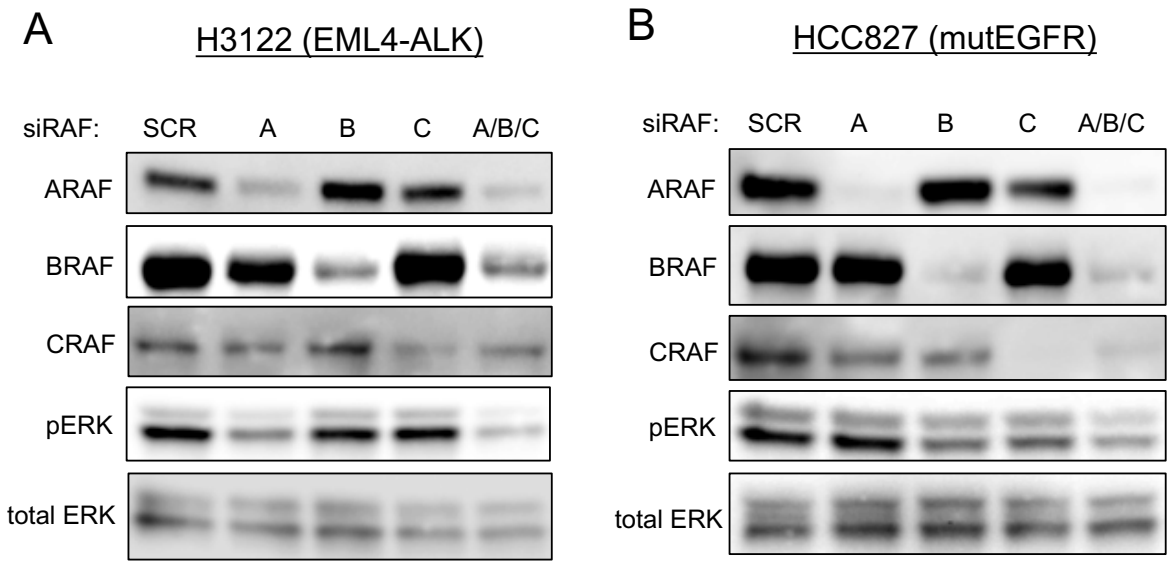

Figure S13: ARAF knockdown reduces MAPK output in oncogenic ALK but not oncogenic EGFR cancer cells. Western blot results from patient-derived EML4-ALK expressing cancer cell line H3122 (A) or EGFR mutant (mutEGFR) cancer cell line HCC827 (B) transfected with siRNA's against either A,B, or C-RAF, all three, or a non-specific scramble siRNA (SCR) for 5 days. Images representative of at least 4 independent replicates and quantification of pERK levels shown in Figures 2G and 2H.

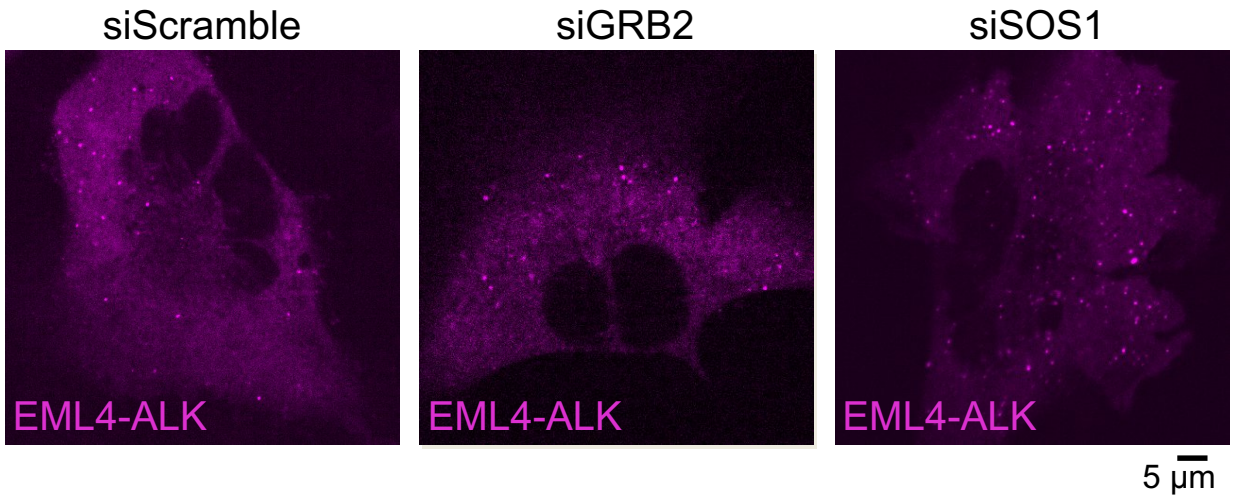

Figure S14: EML4-ALK granules form in the absence of GRB2 or SOS1. Live-cell confocal imaging of human epithelial cell line Beas2B treated with siRNA's against GRB2, SOS1, or control scrambled sequences (siScramble), followed by transfection of mTagBFP2::EML4-ALK after 72 hours. Images are representative of at least 20 cells analyzed per condition in 2 independent replicates.

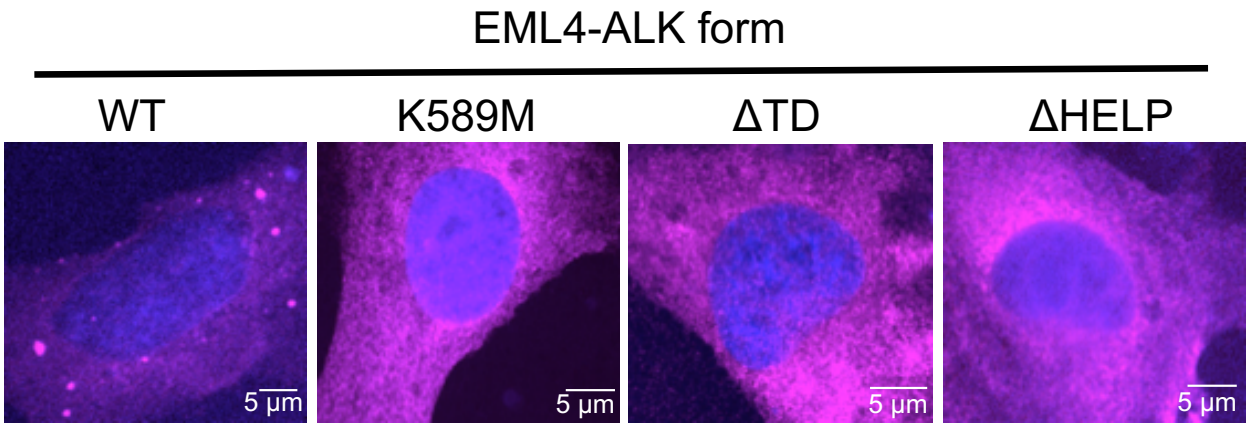

Figure S15: FLAG tagged EML4-ALK mutants do not form cytoplasmic protein granules. Anti-FLAG immunofluorescence of human epithelial cell line Beas2B expressing either FLAG-tagged EML4-ALK wild-type (WT) or EML4-ALK kinase-deficient (K589M), ΔTD or ΔHELP mutants. EML4-ALK (FLAG) staining in pink, DAPI in blue. Images are representative of at least 35 cells analyzed per condition in 2 independent replicates.

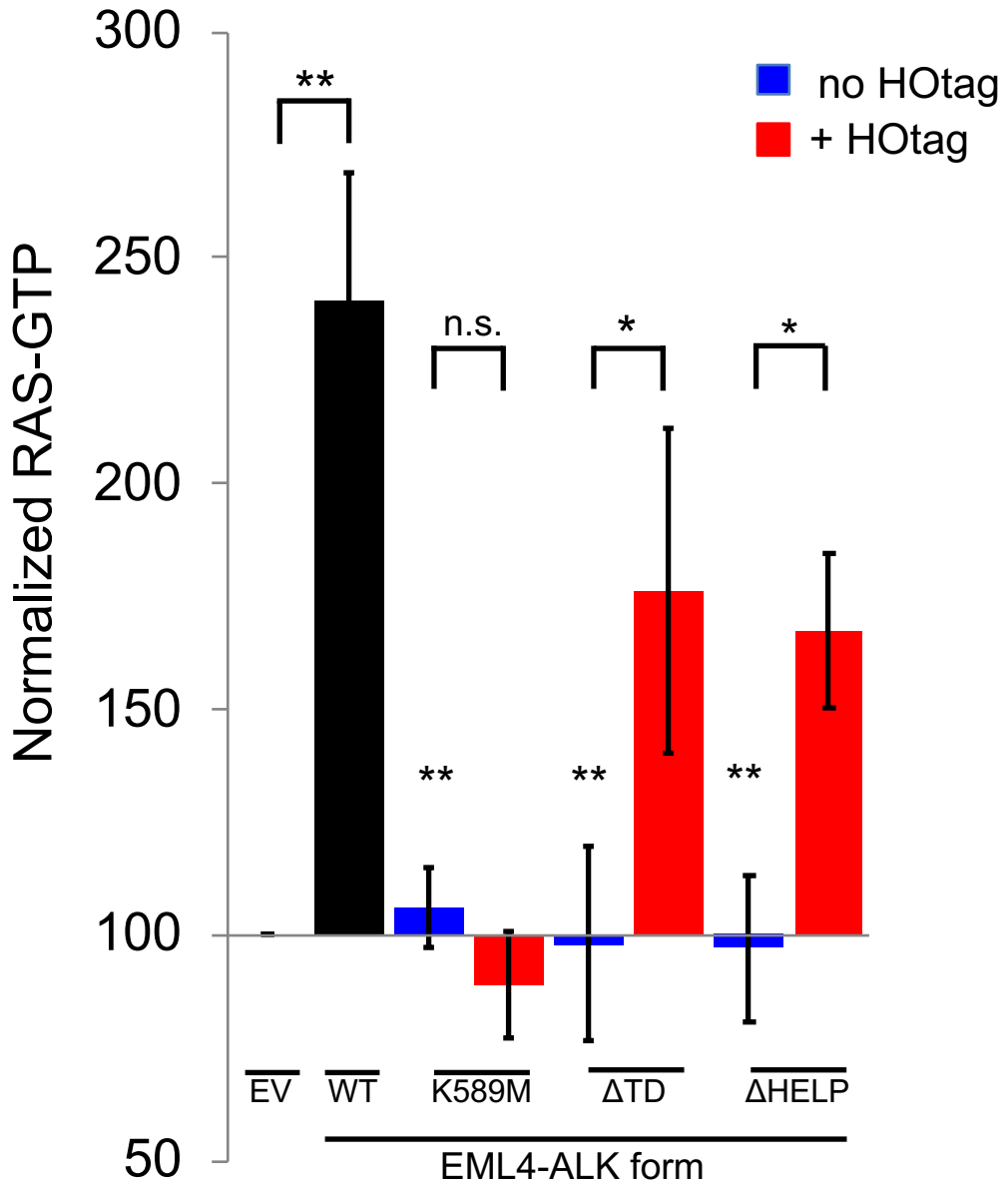

Figure S16: Forced granule formation of EML4-ALK mutants rescues RAS-GTP levels. Assessment of endogenous RAS-GTP levels performed in 293T cells expressing an empty vector (EV), EML4-ALK wild-type (WT), or the diffusely cytoplasmic EML4-ALK mutants (kinase deficient K589M, ΔTD, or ΔHELP) +/– forced clustering (HOtag). EML4-ALK K589M, ΔTD and ΔHELP mutants (blue bars) display significantly reduced RAS-GTP levels compared to wild-type EML4-ALK (black bar), ** denotes $p < 0.01$. Forced clustering (HOtag, red bars) of EML4-ALK ΔTD and ΔHELP mutants, but not EML4-ALK K589M, significantly increases RAS-GTP levels compared to the respective non-clustered EML4-ALK mutants (blue bars), * denotes $p < 0.05$. RAS-GTP levels normalized to total RAS protein levels. N=4. Error bars represent ± SEM, n.s. denotes non-significant comparison.

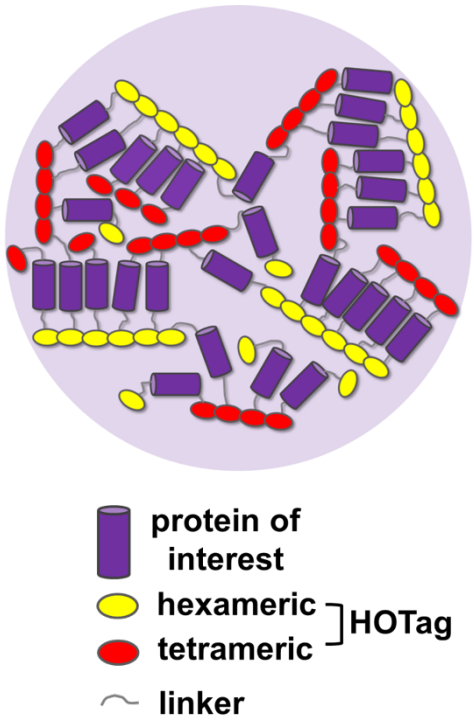

Figure S17: Schematic of HOtag forced clustering system. Forced clustering of proteins achieved by N-terminal hexameric and C-terminal tetrameric tags that form higher ordered clustered assemblies upon expression in cells.

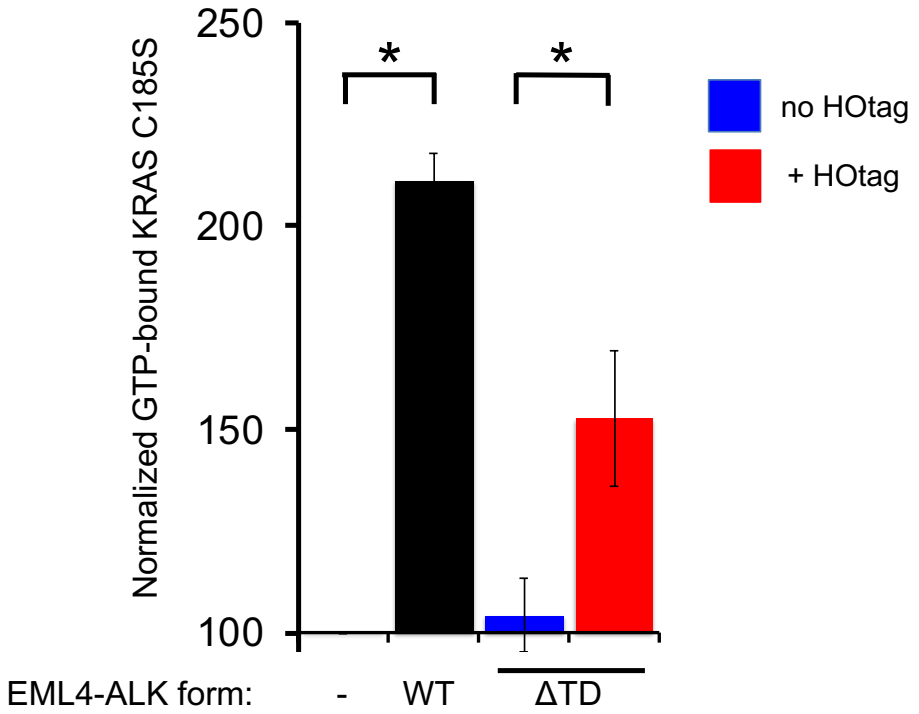

Figure S18: Protein granule dependent activation of cytosolic RAS. Stable expression of cytosolic KRAS mutant (KRAS C185S) in 293T cells, followed by transfection of empty vector (–), EML4-ALK wild-type (WT) or diffusely cytoplasmic EML4-ALK ΔTD mutant +/– forced clustering (HOtag). Levels of GTP-bound KRAS-C185S were normalized to total KRAS C185S protein levels. N=4. Error bars represent ± SEM, * denotes $p < 0.05$.

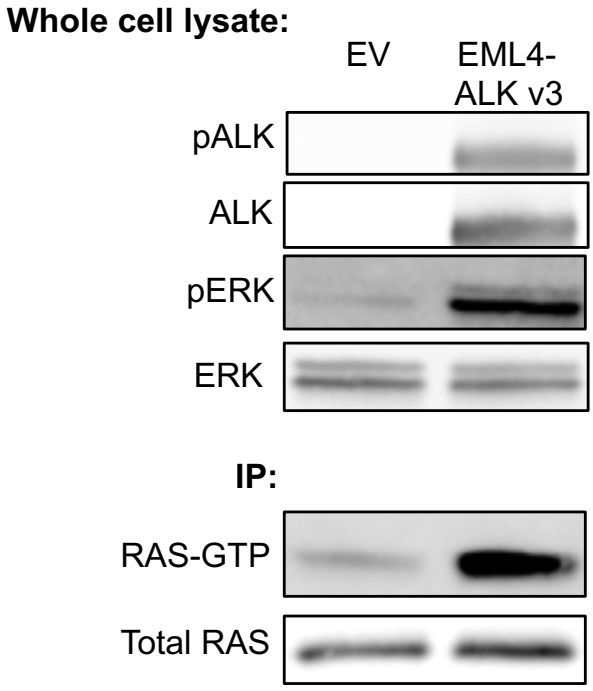

Figure S19: EML4-ALK variant 3 activates RAS-MAPK signaling. Western blot analysis upon expression of empty vector (EV) or EML4-ALK variant 3 in 293T cells to assess levels of EML4-ALK activation (phosphorylation), ERK activation, and in immunoprecipitation (IP) panel, levels of RAS activation (GTP-bound RAS). Representative images from at least 4 independent experiments.

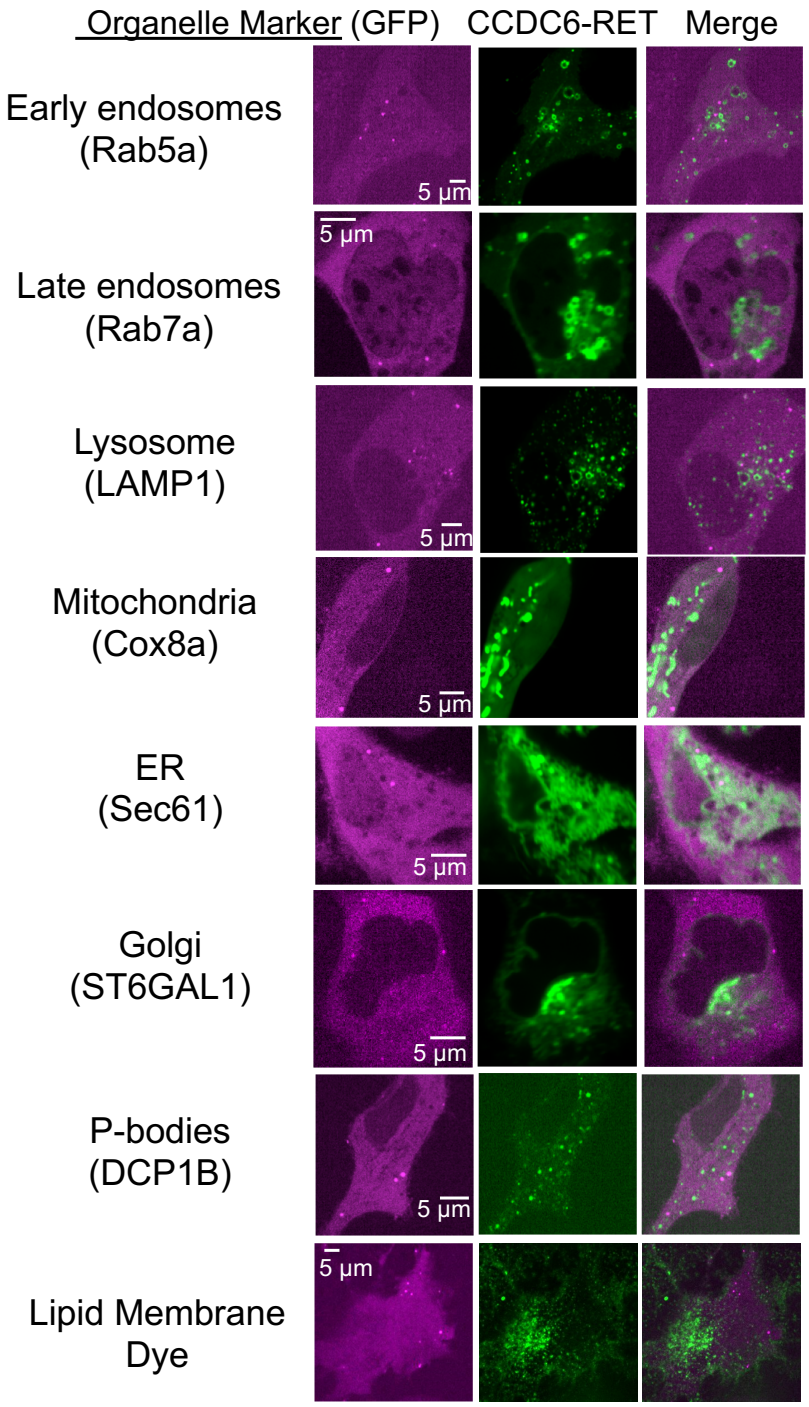

Figure S20: Oncogenic RET granules do not co-localize with lipid membrane containing intracellular structures. Live-cell confocal imaging of human epithelial cell line Beas2B upon expression of mTagBFP2::CCDC6-RET and mEGFP-tagged organelle markers as listed. Membrane dye experiments were conducted using live cells incubated with CellTracker™ CM-DiI Dye (Invitrogen) according to manufacturer's recommended protocol. Each panel is a representative image of at least 20 analyzed cells per condition with at least 2 independent replicates.

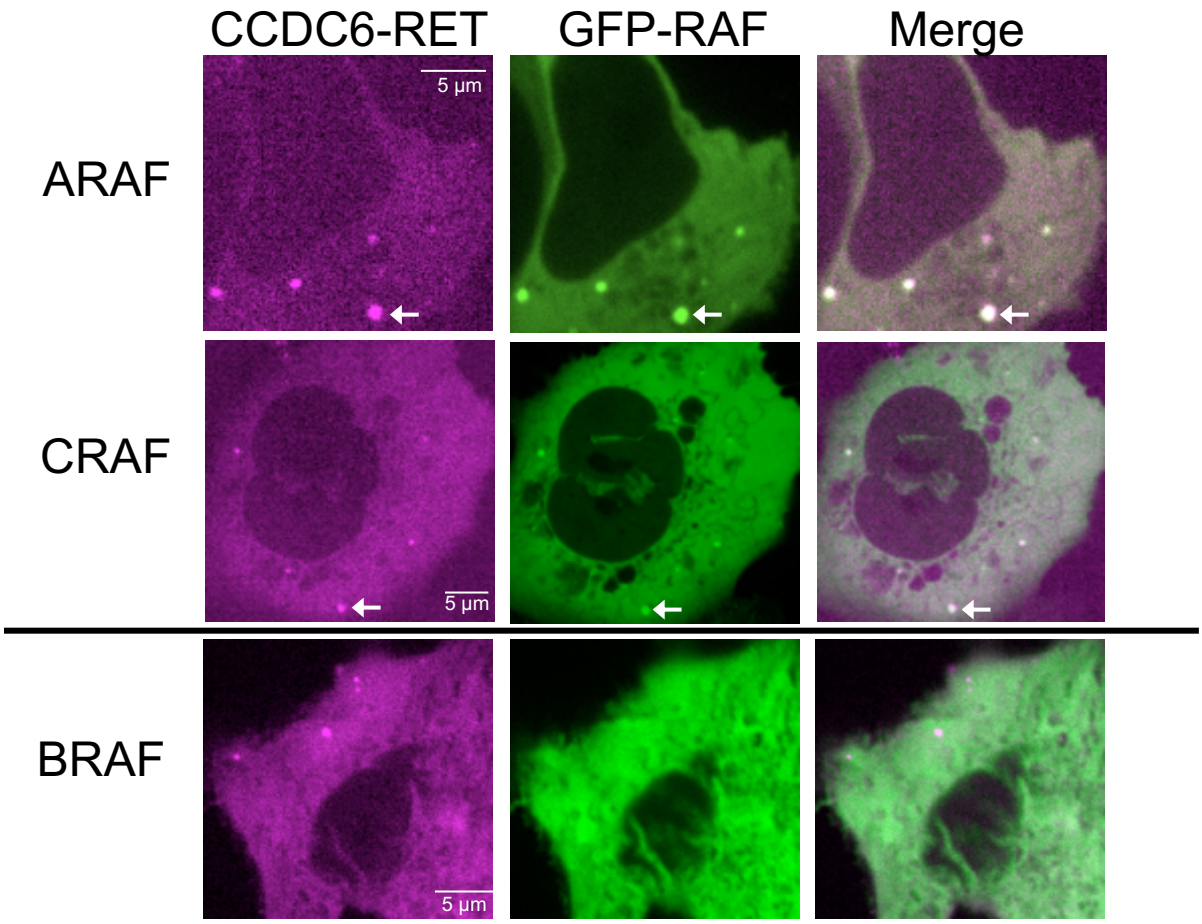

Figure S21: CCDC6-RET granules recruit multiple RAF isoforms in RAS-GTP reporter assay. Live-cell imaging of human epithelial cell line Beas2B expressing mTagBFP2::CCDC6-RET and mEGFP-tagged ARAF, BRAF, or CRAF. White arrows indicate a representative CCDC6-RET cytoplasmic protein granule with local enrichment of ARAF or CRAF (multiple non-highlighted granules also show colocalization between EML4-ALK and ARAF/CRAF). Each panel is a representative image of at least 20 analyzed cells per condition in at least 3 independent experiments.

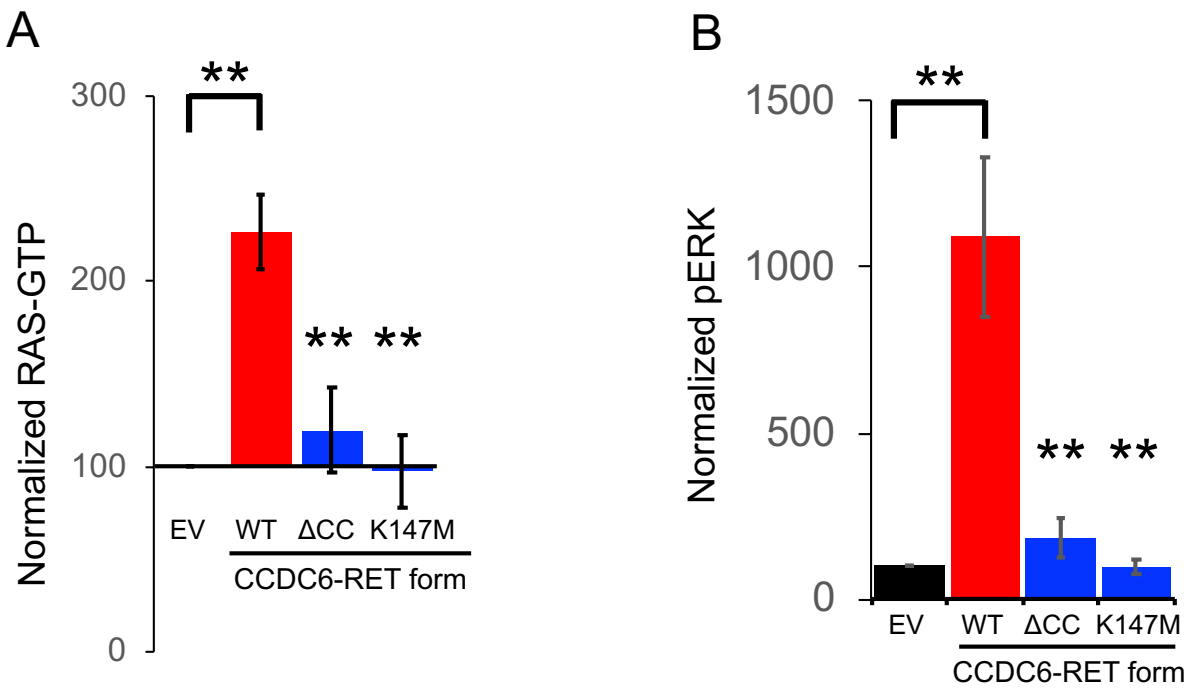

Figure S22: Protein granule formation and RET kinase activity are both necessary for CCDC6-RET to activate RAS/MAPK signaling. (A) Endogenous RAS-GTP levels and (B) ERK phosphorylation were assessed in 293T cells expressing an empty vector (EV), CCDC6-RET wild-type (WT) or CCDC6-RET mutants (ΔCC and kinase-deficient mutant K147M). (A) RAS-GTP levels were normalized to total RAS protein levels, N = 4. (B) pERK levels were normalized to total ERK protein levels, N=5. For both panels, error bars represent ± SEM error, ** denotes $p < 0.01$.

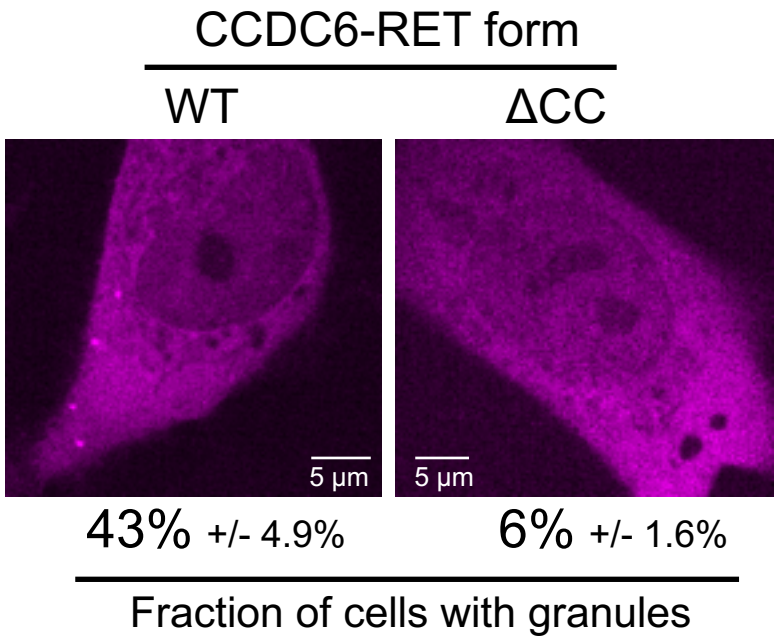

Figure S23: Coiled-coiled domain of CCDC6-RET is required for protein granule formation. Live-cell confocal imaging of human epithelial cell line Beas2B expressing mTagBFP2-labelled CCDC6-RET wild-type (WT) or the coiled-coiled domain deletion mutant (ΔCC). Quantification of cells with 3 or more granules shown as a fraction ± SEM, based on 3 independent experiments of at least 25 cells analyzed per condition.

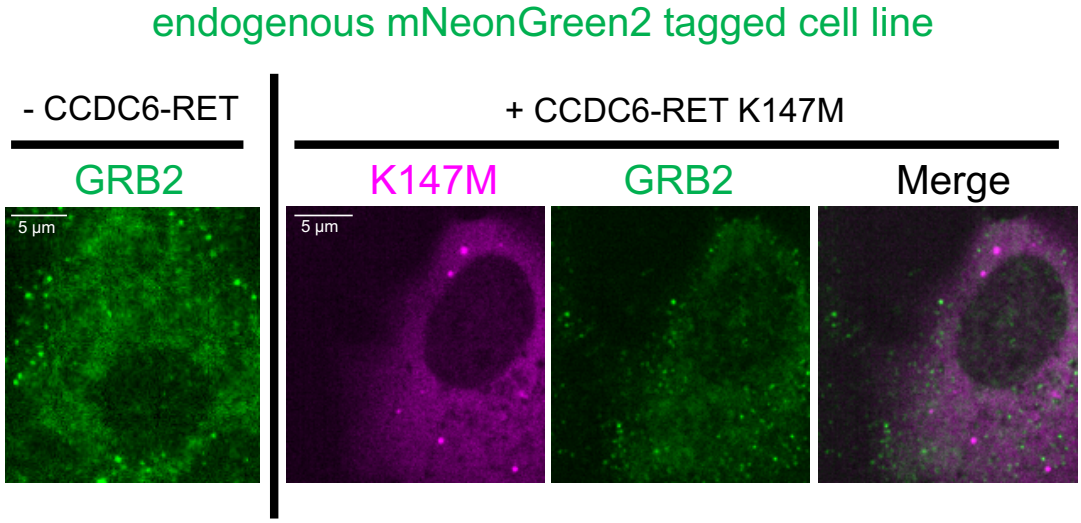

Figure S24: Kinase-deficient CCDC6-RET forms protein granules but does not recruit GRB2. Live-cell confocal imaging of mTagBFP2::CCDC6-RET K147M (kinase-deficient mutant) expressed in the human epithelial cell line Beas2B with endogenous mNeonGreen2-tagging of GRB2. Images are representative of 60 analyzed cells in total over 3 independent experiments with no observed colocalization.